El-Jughrafiyah
Ari Rachmadi, dkk
Volume 04, Issue 02, Tahun 2024

Determination of Liquefaction Hazard in Samarinda Using Fuzzy-GIS Method

Ari Rachmadi[1], Muhammad Rizqy Septyandy[1], Muhammad Amin Syam[1]

[1]*Geologycal Engineering Study Program, Faculty of Engineering, Mulawarman University*
e-mail: arirachmadi75@gmail.com

ABSTRACT. The phenomenon of liquefaction is the transformation of coarse-grained soil from a solid to a liquid state, resulting in a reduction in the bearing capacity of the soil due to an increase in hydrostatic pressure due to a sudden high cyclic load. Liquefaction usually occurs during an earthquake, where earthquake-triggering factors, ground acceleration, water table depth, overburden pressure, soil density, and soil type are used as input data. A fuzzy-GIS approach is used to combine these factors to map liquefaction potential. This method produced a preliminary map of liquefaction potential in Samarinda City. Validation of the Fuzzy-GIS model used field test data to assess liquefaction potential. The technique used in determining the liquefaction hazard zone in Samarinda is fuzzy-GIS processing with the results of field data calculations in CPT tests. The research results are accurate maps of the liquefaction hazard zone of the Samarinda region based on field data validation and Fuzzy-GIS analysis results. Based on the results of this research, the Samarinda area is divided into four zones of liquefaction hazard, ranging from very low to very low and medium to high. This research results in a map of potential liquefaction risk with more than 90% accuracy for prevention and mitigation in Samarinda City.

Key Word: Liquefaction; Hazard; Fuzzy-GIS; Remote Sensing.

INTRODUCTION

Natural disasters can occur at any time and can harm the community with casualties and material and non-material damage (Faizana et al., 2015).Indonesia's number and variety of disasters are the largest in the world. Examples of common natural disasters in Indonesia include tsunamis, earthquakes, floods, and landslides (Santoso et al., 2012). The level of loss that will be received by the general public when a natural disaster occurs is due to the lack of knowledge of possible disasters that could happen and the lack of socialization about mitigation efforts. Therefore, early information on disaster potential and risk is one source that communities can use to provide primary education on disaster response (Yassar et al., 2020)

Most of Indonesia consists of mountainous and hilly areas that are prone to landslides, landslides hit various regions of the country as a result of a number of factors. Basically, the possibility of natural disasters is based on certain natural phenomena, especially in the Indonesian area, which has a geographically complicated landscape. The country lies between three plates of the world: the Indo-Australian, Eurasian and Pacific plates. This causes Indonesia to be in a tectonically active region and allows natural disasters to occur every year (Hardianto et al., 2020).

One of the natural disasters that has come to the attention of the Indonesian people in recent years is liquefaction, which is still a bitter memory of the earthquake in Palu in 2018. During the earthquake, the natural phenomenon of liquefaction also occurred. The event called "liquefaction" occurs when the soil changes from solid to liquid. This event often occurs during earthquakes, when the behavior of the soil is affected by earthquake ground motions that occur for only a short period of time. Earthquake vibrations propagate into soil deposits in a short time, changing the soil mass from a solid state to a liquid state (Hakam, 2020).

In the aftermath of the 2018 Palu earthquake, experts have been conducting research on liquefaction. The earthquake that shook Palu and Donggala in Central Sulawesi on 28 September 2018, also caused a natural phenomenon, namely liquefaction or in the local language called "nalodo". Thousands of houses were affected by liquefaction, especially in the Petobo and Balaroa areas. The possibility of liquefaction is closely related to the phreatic depth phenomenon. Groundwater exists in rocks within geological basins. A groundwater basin is a hydrogeological system that consists of one or more interconnected aquifer sections and forms a system that can change due to environmental changes. A groundwater basin is an area where water originates from surface runoff. Quantitative estimation of water resources is essential and can be achieved through adsorption and water balance techniques (Zeffitni et al., 2020).

Experts have been researching liquefaction in the aftermath of the 2018 Palu earthquake. The earthquake that shook Palu and Donggala in Central Sulawesi on 28 September 2018 also caused a natural phenomenon, namely liquefaction or, in the local language, "nalodo." Thousands of houses were affected by liquefaction, especially in the Petobo and Balaroa areas. The possibility of liquefaction is closely related to the phreatic depth phenomenon. Groundwater exists in rocks within geological basins. A groundwater basin is a hydrogeological system that consists of one or more interconnected aquifer sections and forms a system that can change due to environmental changes. A groundwater basin is an area where water originates from surface runoff. Quantitative estimation of water resources is essential and can be achieved through adsorption and water balance techniques (Zeffitni et al., 2020).

The phenomenon of liquefaction became a disaster that received widespread attention from academics and the general public worldwide when, on 28 September 2018, three geological disasters occurred close to each other, namely earthquakes, tsunamis, and liquefaction. This phenomenon seemed to open the eyes of public officials and related institutions or agencies to act quickly to map the condition of their area, significantly associated with the liquefaction potential. This condition is based on the fact that the disaster in Palu caused the most losses, casualties, and damage due to liquefaction. Earthquakes are relatively rare on the island of Kalimantan, especially in Samarinda. However, on 5 June 2015, there was an earthquake in Ranau, Sabah, Malaysia, with a magnitude of 6.0 Mw. This earthquake resulted in 19 fatalities, landslides on Mount Kinabalu, and several damaged buildings in Ranau City. Based on BMKG records, before the earthquake in Ranau City, there was also an earthquake with a magnitude of 5.7 Mw on 25 February 2015, with the epicenter located 413 km northeast of Tarakan City (PUSGEN, 2017). This condition indicates that Kalimantan, or the city of Samarinda, is not entirely safe from earthquakes, as citizens understand, due to its proximity to the Mangkalihat Fault Zone located north of the city.Liquefaction is an additional event after an earthquake, especially in earthquake-affected sites with liquefiable soils, such as saturated silty sands and non-cohesionless sands. In most liquefaction cases reported in the literature, the shear strength of the liquefaction layer is almost zero, and the pore water pressure increases beyond normal levels. Infrastructure is usually damaged after an earthquake shakes the ground (Agung et al., 2023).

Liquefaction events can cause the soil to change properties, such as losing strength and stiffness, and becoming liquid-like. After an earthquake occurs, the water pressure in the soil is rather low. However, after the tremor, the water pressure increases, allowing soil particles to move easily (Hutagalung & Tarigan, 2019). Liquefaction can be affected by surrounding conditions. Liquefaction potential is influenced by several factors. One of them is the location close to the presence of faults, as well as water areas (sea, beach, etc.) (Agustian, 2021).

In-depth research into liquefaction processes, especially those that have occurred in Palu and the surrounding region, is still being conducted. However, this simple research does not go into the details of the complex liquefaction formula. Simple experiments are used in this research to explain the mechanism of liquefaction so that general people who are not directly involved in geology, soil mechanics, seismicity, or other disciplines related to the liquefaction phenomenon can

understand it. The damage caused by the liquefaction phenomenon can be reduced with this simple understanding (Agustian, 2021).

During a liquefaction situation, the soil will not be able to withstand the load from the superstructure. After the earthquake, soil deposits will liquefy, causing significant cyclic damage. The change from solid to liquid state of granular materials, caused by the increase of water pressure and reduction of effective stress, is known as softening. The ratio of excess pore water pressure affects the decrease of effective stress in soil deposits. Researchers investigating liquefaction use experimental studies of the parameters. Many researchers perform analyses empirically such as experimental liquefaction. Soil condition to seismic response is an additional factor that can affect liquefaction. Soil engineering properties, geological conditions, and seismicity significantly affect liquefaction (Jalil et al., 2020).

Liquefaction safety using field investigation data such as CPT, SPT, and shear wave velocity (VS) is the most common analysis performed in liquefaction. Cyclic Resistance Ratio (CRR) and Cyclic Stress Ratio (CSR) are compared to perform the analysis. This analysis is easy to use, practical, and widely used by researchers worldwide. Although this method is commonly used in studying liquefaction, it does not describe the actual condition approach. While predicting excess pore water pressure is difficult, this method only considers cyclic stress and resistance. The result of this technique is a factor of safety. Experimental research is preferred to study liquefaction. This research is especially proper for dynamic tests such as cyclic triaxial, shaking table, and simple cyclic shear. The excess pore water pressure ratio is used to measure liquefaction in these tests. This idea is more reliable for measuring liquefaction potential. It is strongly related to excessive pressure in pore water, which can cause liquefaction (Mase, 2017).

Factors that can cause liquefaction include strong earthquake shaking that can damage the grain structure of the soil, sandy soil (loose sand), water-saturated soil (saturated soil), and shallow water table are some of the soil types that are prone to liquefaction. Soil improvement with stone columns is one of the soil improvement methods that can increase the bearing capacity of the soil, reduce the settlement of structures built on it, increase strength, reduce compressibility in fine-graded soils, accelerate consolidation, and reduce the potential for soil liquefaction (Fajarwati & Kusuma, 2021). Samarinda City is tectonically located in the Kutai Basin. The Kutai Basin is the largest and deepest basin in Indonesia located on the east coast of Kalimantan Island. The basin formed and developed as a result of strain-induced secession processes within the Sunda Microplate that accompanied the interaction between the Sunda plate and the Pacific plate to the east, the Indo-Australian plate to the south, and the South China Sea plate to the north (Allen & Chambers, 1998).

Liquefaction events often occur in conjunction with earthquakes. This can happen because during an earthquake the soil loses its strength and receives a heavy load on it, so that when the soil pores are saturated with groundwater content, liquefaction will occur. Kalimantan is an island that is often considered safe from natural disasters. But in fact, Kalimantan Island has three main fault zones that have been identified from previous research, namely the Tarakan, Mangkalihat, and Meratus Fault zones. The following is an illustration of the location of the three active faults. Tectonically, to the north of the Kutai Basin is the Tarakan Basin which is separated by the Mangkalihat Ridge. This ridge is an area of bedrock uplift formed in the Oligocene epoch. To the south is the Barito Basin which is bounded by the Adang Fault, which was formed in the Middle Miocene. In the southeast there is the Patenoster Plain and the Meratus Mountains group, while the western boundary is the Kuching Plateau area (Central Kalimantan Mountains) which is Pre-Tertiary in age and is part of the continental core of Kalimantan Island where this plateau produces thick Neogene sediments, which can be seen in **Figure 1** (Darman & Sidi, 2000)

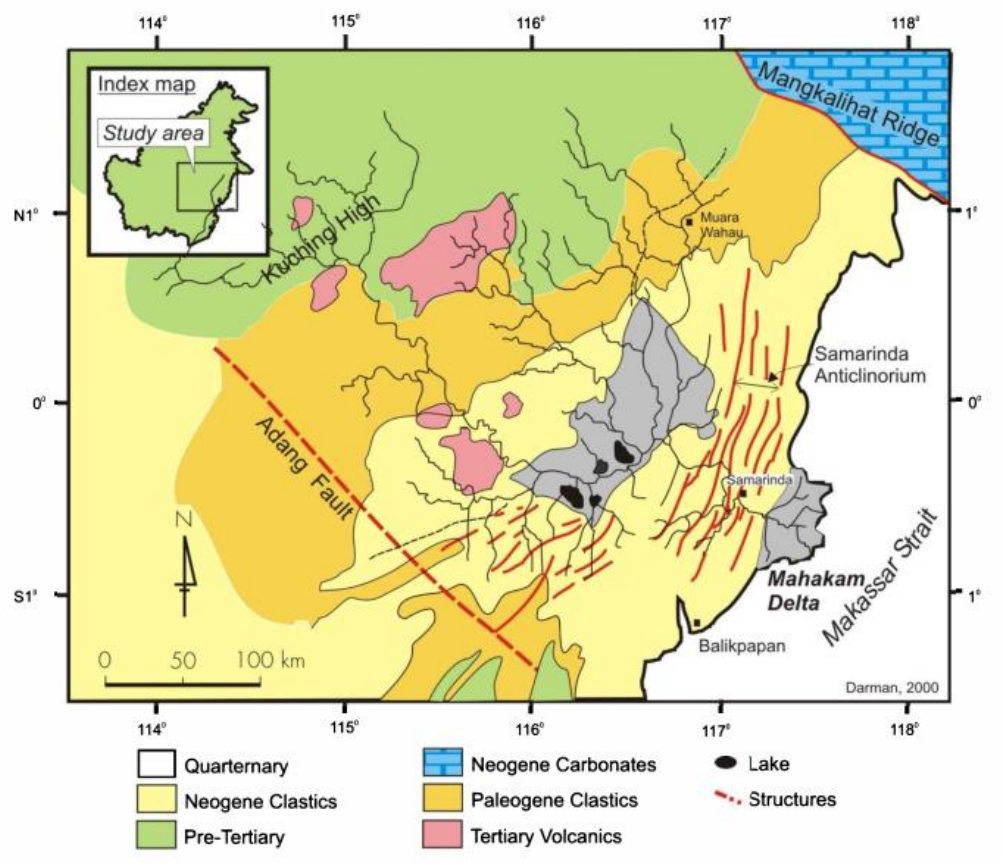

Figure 1. Peta geologi regional Cekungan Kutai (Darman & Sidi, 2000)

METHODOLOGY

This research aims to conduct modeling of liquefaction vulnerability zones and provide information on areas that have a vulnerability to liquefaction in Samarinda City. It is hoped that the research results can be used as a reference in carrying out mitigation efforts, and they are expected to minimize the impact that will occur if there is a disaster in the Samarinda City area.

One way to investigate soils in situ is by cone penetration test (CPT)/sondir. This method can be very effective in identifying the material properties of soils at the study site, especially those with unconsolidated stratigraphic layers, soft materials, discontinuous lenses, organic materials (peat), and potentially liquefiable materials. Many people now use electric piezocone and slip cones for CPT, which refer to ASTM D-5778. By using the CPT test in the field, it is possible to determine the soil layer and type using a graph based on the cone resistence and sleeve friction values (Arya et al., 2018).

Cone Penetration Test (CPT) has proven to be a valuable tool in characterizing subsurface conditions and in assessing various soil properties, including estimating liquefaction potential at specific sites (Idriss and Boulanger, 2008). The main advantage of using CPT is that it provides a record of sustained penetration and is less prone to operator error than tests using the Standard Penetration Test (SPT), while the main disadvantage is that the CPT cannot sample the soil when measuring soil strength (Boulanger et al., 2014).

In this study, data were taken from the results of field tests (CPT) and secondary data in the field data collection stage using the CPT (Cone Penetration Test) method. From the results of CPT field data that has been carried out, calculations can be made using existing parameters to determine the liquefaction potential of an area. The CPT data is then processed to obtain the liquefaction potential value of the area (LPI). Then, it is analyzed and correlated with secondary data in the form

of PGA (Peak Ground Acceleration) data, vs30, groundwater level, lithology type, soil type, and slope as map input, which will be combined and overlaid to become a map of liquefaction vulnerability. This research was conducted using field test data and input map data. From the results of the CPT field data that has been carried out, calculations can be made using existing parameters to determine the liquefaction potential of an area.

Fuzzy logic is a technique that does not use number variables but only language variables that are used to find specific locations and correspond to predetermined variables. To analyze the interaction relationship between all sets and combine membership requires a fuzzy overlay tool. Fuzzy overlay serves to calculate the possibility of each cell or location to produce a certain set based on the membership value. This stage requires operators in the process, these operators can return fuzzy values derived from the combination of fuzzy sets, the results of these values depend on the operator used. Each of them provides a different aspect in explaining the relationship between membership cells and input cells.

1. Fuzzy AND is an operator that produces the smallest (minimum) fuzzymember value from some input data.
2. Fuzzy Or, this fuzzy operator produces the maximum value of fuzzy members from some input data to produce a given location.
3. Fuzzy Product, for each cell, multiply each fuzzy value for all input criteria. The resulting product will be smaller than any of the inputs, and when members from many sets are included, the value can be very small.
4. Fuzzy Sum, will add the fuzzy values from each set of cell locations. The resulting sum is an increasing linear combination function that is based on the number of criteria entered into the analysis.
5. Fuzzy Gamma operator is a combination of Fuzzy Algebraic Product and Algebraic Sum. When combined, they will produce a value between the two possibilities, which is controlled by the number of gamma parameters used.

.(Indra et al., 2013)

Fuzzy Overlay is a part of geographic information system software used for the analysis of variables belonging to several sets in multicriteria. Each approach can provide different aspects of the parameters of each cell with multiple criteria. The fuzzy overlay feature in geographic information system software is used to analyze variables in multicriteria sets. Each method can provide different aspects of the parameters of each Fuzzy Overlay. It allows the analysis of relationships between parameters by combining data based on set theory analysis. It is based on fuzzy logic theory, which defines membership by using a Gaussian function for each input raster rather than providing a specific judgment for the overlay weighting function Fuzzy Overlay is able to analyze the relationship between several parameters by combining data based on set theory analysis. This is based Fuzzy Logic theory that defines membership using a Gaussian function on each input raster rather than assigning individual ratings in the weighting overlay function function on each input raster rather than assigning individual ratings in a weighted overlay function.(Wijayanto, 2020)

This fuzzy analysis method combines several maps as inputs, which will then be given weight values and processed to be combined into a map output, namely the map of the liquefaction vulnerability of the research area. This study uses fuzzy overlay to model multi-criteria spatial data. The fuzzy logic theory provides an exceptional judgment about the weighting overlay function, and the fuzzy overlay produces more accurate results in the level of suitability by comparing the results of the weighting overlay. The following is a flowchart of the research method, which can be seen in **Figure 2.**

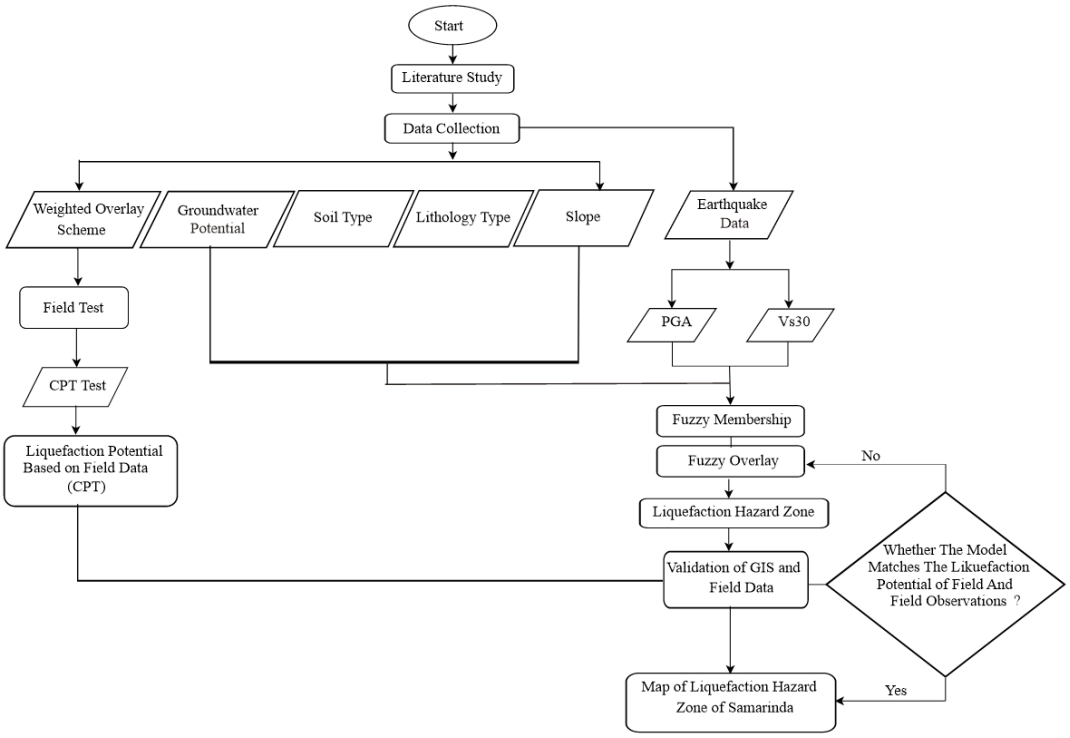

Figure 2. Research Flowchart.

1. Cone Penetration Test

Before conducting the CPT test in the field, a weighting scheme of several input data was made to determine the point that has a liquefaction hazard. This weighting scheme uses weighted overlay in Arcgis. At this stage 3 schemes were made that adjusted the score of the existing input data. There are 5 input data, namely contours, groundwater potential, PGA, soil type, and lithology type. In scheme one, all input data were given the same score, which is 20%. In scheme 2 PGA 35%, groundwater potential 35%, lithology type 10%, soil type 10%, and contour 10%. In scheme 3 PGA 30%, groundwater potential 30%, lithology type 20%, soil type 10%, and contour 10%. The following is a comparison of the schemes generated by the 3 schemes that have been created.

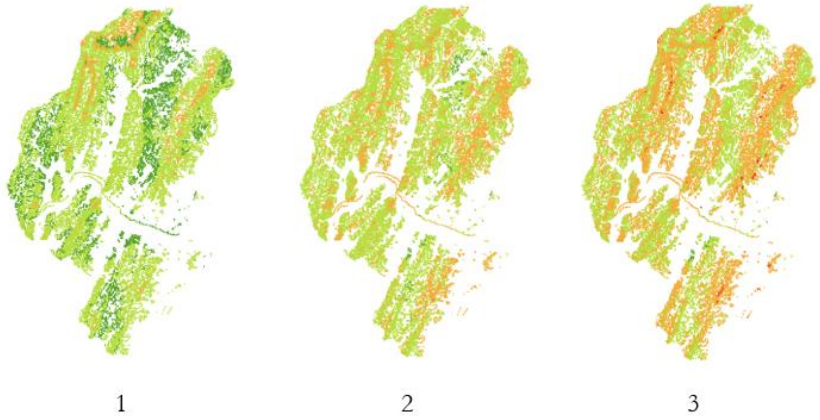

Figure 3. Comparison of 3 Weighted Overlay Schemes

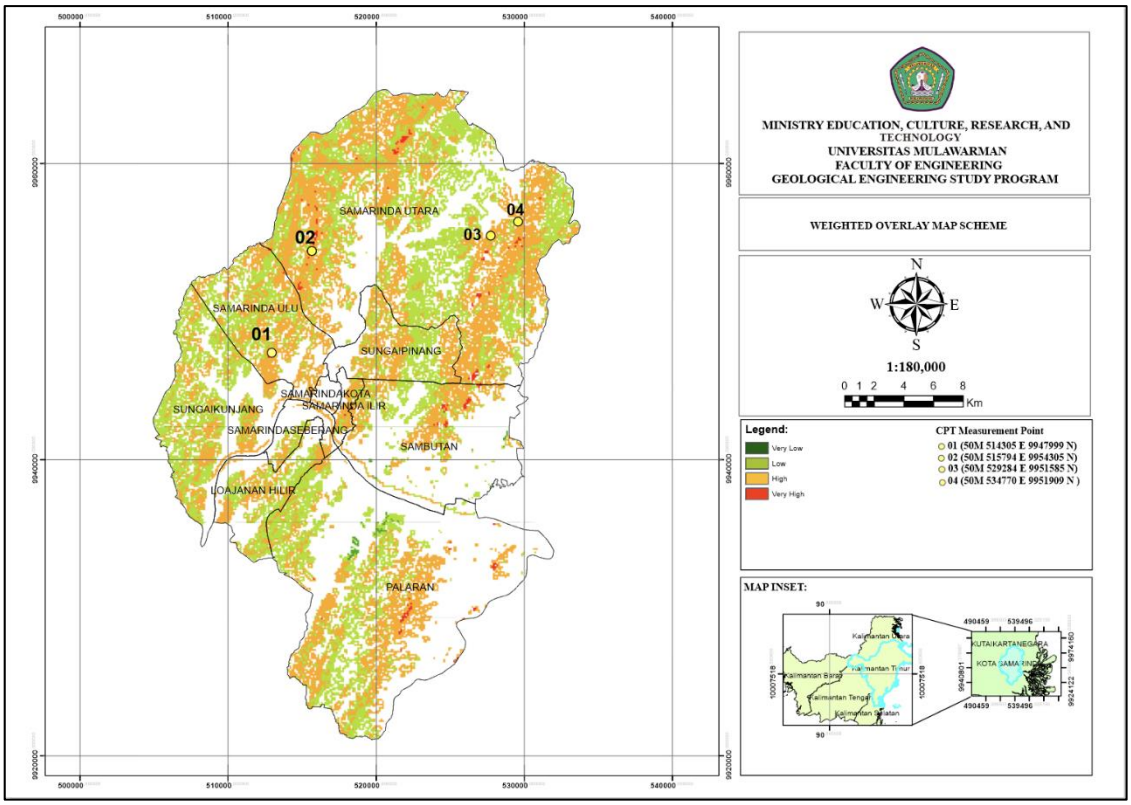

Figure 4. Map of weighted overlay scheme and CPT test point locations.

Based on **Figure 3** that have been made, scheme 3 was chosen, because only scheme 3 presents weighting results that have red or high points based on the percentage of input data that has been set at 30% PGA, 30% groundwater potential, 20% lithology type, 10% soil type and 10% contour. After the selection of scheme 3 as a reference for determining the CPT test point, the CPT test in the field is carried out at the orange-red color point. The following is a map of CPT test point locations based on scheme 3 that has been made.

After obtaining a reference point for the location to be carried out CPT, then CPT is carried out at 4 existing points and represents the red dot of the weighted overlay scheme map which can be seen in **Figure 4.** Measurements were taken at 4 points. the first measurement point is located at coordinates 513131°E 9947546°N located in Air Putih Village, Samarinda Ulu District, Samarinda City. At the point the conus reached a depth of 7.4m. At this location the type of soil density Hard / Hard is obtained to a depth of 7.40 m. The second point is located at coordinates 515794°E 9954305°N located in Sempaja Utara Village, North Samarinda District, Samarinda City. At point 2 the cone reaches a depth of 1.4m. The third point is located at coordinates 527674°E 9955333°N located in Sungai Siring Village, North Samarinda Subdistrict, Samarinda City. At point 3 the cone reaches a depth of 7m. The fourth point is located at coordinates 529495°E 9956267°N located in Sungai Siring Village, North Samarinda Subdistrict, Samarinda City. At point 4 the cone reaches a depth of 1m.

The results of CPT measurements at the four points stated the results of different depths and conus readings, this occurred due to the influence of different soil hardness at the 4 points. at locations that have relatively soft soil will get deep enough CPT measurement results, while at measurement locations that have hard soil characteristics only get a depth of less than 2m. the results of the 4-point measurement can be seen in **Table.1** the following CPT measurement results.

Table 1. Table of CPT measurement results at point 1-4

CV. PRISMA SOENOE
SOIL TEST, SONDIR,BORING, SPT, SURVEY PEMETAAN & LABORATORIUM
OFFICE : Jl. Kemuning No.24 Rt.02 Tlp : (0541) 272508
: Jl. Jakarta Blok BE No.24 RT.58 Loa Bakung Tlp : (0541) 270783
Samarinda Kalimantan Timur
BILKEV SERTIFIKASI INDONESIA
ISO 14001:2015 ISO 9001 :2015 ISO 45001:2018

DUTCH CONE PENETROMETER TEST

DCPT No. : S.01 (X:0513131; Y:9947546)
PROJECT : Uji Potensi Likuifaksi Daerah Samarinda
LOCATION : Gunung Batu, Kel. Air Putih, Kota Samarinda
G. W. Level : -
Date Commenced : 19 September 2023
DCPT Type : Sondir Manual
Soil Test Technician : Supiansyah & Team
Soil Mec. Engineer : Isnawati Am.d

DEPTH (Meter)	Manometer Reading 1st M_1 (Kg/cm²)	Manometer Reading 2nd M_2 (Kg/cm²)	Compressive Strength Cone Resistance $M_1.C_2$ (Kg/cm²)	Compressive Strength Local Resistance $(M_2-M_1).C_1$ (Kg/cm²)	Total resistance $HL=(M_2-M_1).C_2.L/l$ (Kg/cm)	Accumulative JHL = ΣHL (Kg/cm)	Friction Ratio (%)
0,00	0,00	0,00	0,00	0,00000	0,00	0,00	0,00
20	6,00	8,00	5,93	0,17525	3,51	3,51	2,95
40	8,00	11,00	7,91	0,26288	5,26	8,76	3,32
60	10,00	13,00	9,89	0,26288	5,26	14,02	2,66
80	13,00	16,00	12,86	0,26288	5,26	19,28	2,04
1,00	15,00	20,00	14,83	0,43813	8,76	28,04	2,95
20	17,00	22,00	16,81	0,43813	8,76	36,80	2,61
40	20,00	25,00	19,78	0,43813	8,76	45,57	2,22
60	23,00	28,00	22,74	0,43813	8,76	54,33	1,93
80	27,00	34,00	26,70	0,61339	12,27	66,60	2,30
2,00	32,00	40,00	31,64	0,70101	14,02	80,62	2,22
20	34,00	43,00	33,62	0,78864	15,77	96,39	2,35
40	36,00	45,00	35,60	0,78864	15,77	112,16	2,22
60	38,00	47,00	37,58	0,78864	15,77	127,93	2,10
80	39,00	48,00	38,57	0,78864	15,77	143,71	2,04
3,00	40,00	50,00	39,55	0,87627	17,53	161,23	2,22
20	45,00	59,00	44,50	1,22677	24,54	185,77	2,76
40	50,00	65,00	49,44	1,31440	26,29	212,06	2,66
60	58,00	73,00	57,35	1,31440	26,29	238,34	2,29
80	65,00	81,00	64,28	1,40202	28,04	266,38	2,18
4,00	70,00	88,00	69,22	1,57728	31,55	297,93	2,28
20	65,00	81,00	64,28	1,40202	28,04	325,97	2,18
40	55,00	70,00	54,39	1,31440	26,29	352,26	2,42
60	50,00	65,00	49,44	1,31440	26,29	378,55	2,66
80	45,00	59,00	44,50	1,22677	24,54	403,08	2,76
5,00	40,00	50,00	39,55	0,87627	17,53	420,61	2,22
20	45,00	59,00	44,50	1,22677	24,54	445,14	2,76
40	50,00	65,00	49,44	1,31440	26,29	471,43	2,66
60	55,00	70,00	54,39	1,31440	26,29	497,72	2,42
80	60,00	75,00	59,33	1,31440	26,29	524,01	2,22
6,00	65,00	81,00	64,28	1,40202	28,04	552,05	2,18
20	75,00	95,00	74,16	1,75253	35,05	587,10	2,36
40	85,00	105,00	84,05	1,75253	35,05	622,15	2,09
60	105,00	125,00	103,83	1,75253	35,05	657,20	1,69
80	135,00	155,00	133,50	1,75253	35,05	692,25	1,31
7,00	175,00	200,00	173,05	2,19066	43,81	736,06	1,27
20	210,00	235,00	207,66	2,19066	43,81	779,88	1,05
40	253,00	278,00	250,18	2,19066	43,81	823,69	0,88
60							
80							
8,00							
20							
40							
60							
80							
9,00							
20							
40							
60							
80							
10,00							
20							
40							
60							
80							

CV. PRISMA SOENOE
SOIL TEST, SONDIR,BORING, SPT, SURVEY PEMETAAN & LABORATORIUM
OFFICE : Jl. Kemuning No.24 Rt.02 Tlp : (0541) 272508
: Jl. Jakarta Blok BE No.24 RT.58 Loa Bakung Tlp : (0541) 270783
Samarinda Kalimantan Timur
BILKEV SERTIFIKASI INDONESIA
ISO 14001:2015 ISO 9001 :2015 ISO 45001:2018

DUTCH CONE PENETROMETER TEST

DCPT No. : S.02 (X:0515794; Y:9954305)
PROJECT : Uji Potensi Likuifaksi Daerah Samarinda
LOCATION : Gunung Batu Cermin, Kel. Sempaja Utara, Kota Samarinda
G. W. Level : -
Date Commenced : 19 September 2023
DCPT Type : Sondir Manual
Soil Test Technician : Supiansyah & Team
Soil Mec. Engineer : Isnawati Am.d

DEPTH (Meter)	Manometer Reading 1st M_1 (Kg/cm²)	Manometer Reading 2nd M_2 (Kg/cm²)	Compressive Strength Cone Resistance $M_1.C_2$ (Kg/cm²)	Compressive Strength Local Resistance $(M_2-M_1).C_1$ (Kg/cm²)	Total resistance $HL=(M_2-M_1).C_2.L/l$ (Kg/cm)	Accumulative JHL = ΣHL (Kg/cm)	Friction Ratio (%)
0,00	0,00	0,00	0,00	0,00000	0,00	0,00	0,00
20	10,00	13,00	9,89	0,26288	5,26	5,26	2,66
40	32,00	40,00	31,64	0,70101	14,02	19,28	2,22
60	75,00	95,00	74,16	1,75253	35,05	54,33	2,36
80	130,00	150,00	128,55	1,75253	35,05	89,38	1,36
1,00	180,00	205,00	177,99	2,19066	43,81	133,19	1,23
20	210,00	235,00	207,66	2,19066	43,81	177,01	1,05
40	254,00	279,00	251,17	2,19066	43,81	220,82	0,87
60							
80							
2,00							
20							
40							
60							
80							
3,00							
20							
40							
60							
80							
4,00							
20							
40							
60							
80							
5,00							
20							
40							
60							
80							
6,00							
20							
40							
60							
80							
7,00							
20							
40							
60							
80							
8,00							
20							
40							
60							
80							
9,00							
20							
40							
60							
80							
10,00							
20							
40							
60							
80							

CV. PRISMA SOENOE
SOIL TEST, SONDIR,BORING, SPT, SURVEY PEMETAAN & LABORATORIUM
OFFICE : Jl. Kemuning No.24 Rt.02 Tlp : (0541) 272508
: Jl. Jakarta Blok BE No.24 RT.58 Loa Bakung Tlp : (0541) 270783
Samarinda Kalimantan Timur
BILKEV SERTIFIKASI INDONESIA
ISO 14001:2015 ISO 9001 :2015 ISO 45001:2018

DUTCH CONE PENETROMETER TEST

DCPT No. : S.03 (X:0527674; Y:9955333)
PROJECT : Uji Potensi Likuifaksi Daerah Samarinda
LOCATION : Jl. Bukit Seribu, Kel. Sungai Siring, Kota Samarinda
G. W. Level : -
Date Commenced : 20 September 2023
DCPT Type : Sondir Manual
Soil Test Technician : Supiansyah & Team
Soil Mec. Engineer : Isnawati Am.d

DEPTH (Meter)	Manometer Reading 1st M_1 (Kg/cm²)	Manometer Reading 2nd M_2 (Kg/cm²)	Compressive Strength Cone Resistance $M_1.C_2$ (Kg/cm²)	Compressive Strength Local Resistance $(M_2-M_1).C_1$ (Kg/cm²)	Total resistance $HL=(M_2-M_1).C_2.L/l$ (Kg/cm)	Accumulative JHL = ΣHL (Kg/cm)	Friction Ratio (%)
0,00	0,00	0,00	0,00	0,00000	0,00	0,00	0,00
20	10,00	13,00	9,89	0,26288	5,26	5,26	2,66
40	15,00	20,00	14,83	0,43813	8,76	14,02	2,95
60	20,00	25,00	19,78	0,43813	8,76	22,78	2,22
80	25,00	30,00	24,72	0,43813	8,76	31,55	1,77
1,00	32,00	40,00	31,64	0,70101	14,02	45,57	2,22
20	25,00	30,00	24,72	0,43813	8,76	54,33	1,77
40	20,00	25,00	19,78	0,43813	8,76	63,09	2,22
60	15,00	20,00	14,83	0,43813	8,76	71,85	2,95
80	12,00	15,00	11,87	0,26288	5,26	77,11	2,22
2,00	10,00	13,00	9,89	0,26288	5,26	82,37	2,66
20	14,00	18,00	13,84	0,35051	7,01	89,38	2,53
40	18,00	23,00	17,80	0,43813	8,76	98,14	2,46
60	22,00	27,00	21,75	0,43813	8,76	106,90	2,01
80	26,00	32,00	25,71	0,52576	10,52	117,42	2,04
3,00	30,00	37,00	29,67	0,61339	12,27	129,69	2,07
20	32,00	40,00	31,64	0,70101	14,02	143,71	2,22
40	34,00	43,00	33,62	0,78864	15,77	159,48	2,35
60	36,00	45,00	35,60	0,78864	15,77	175,25	2,22
80	38,00	47,00	37,58	0,78864	15,77	191,03	2,10
4,00	40,00	50,00	39,55	0,87627	17,53	208,55	2,22
20	45,00	59,00	44,50	1,22677	24,54	233,09	2,76
40	50,00	65,00	49,44	1,31440	26,29	259,37	2,66
60	57,00	72,00	56,36	1,31440	26,29	285,66	2,33
80	65,00	81,00	64,28	1,40202	28,04	313,70	2,18
5,00	70,00	88,00	69,22	1,57728	31,55	345,25	2,28
20	80,00	100,00	79,11	1,75253	35,05	380,30	2,22
40	90,00	110,00	89,00	1,75253	35,05	415,35	1,97
60	100,00	120,00	98,89	1,75253	35,05	450,40	1,77
80	115,00	135,00	113,72	1,75253	35,05	485,45	1,54
6,00	130,00	150,00	128,55	1,75253	35,05	520,50	1,36
20	145,00	165,00	143,38	1,75253	35,05	555,55	1,22
40	160,00	180,00	158,22	1,75253	35,05	590,60	1,11
60	180,00	205,00	177,99	2,19066	43,81	634,42	1,23
80	200,00	225,00	197,77	2,19066	43,81	678,23	1,11
7,00	255,00	280,00	252,16	2,19066	43,81	722,04	0,87
20							
40							
60							
80							
8,00							
20							
40							
60							
80							
9,00							
20							
40							
60							
80							
10,00							
20							
40							
60							
80							

CV. PRISMA SOENOE
SOIL TEST, SONDIR,BORING, SPT, SURVEY PEMETAAN & LABORATORIUM
OFFICE : Jl. Kemuning No.24 Rt.02 Tlp : (0541) 272508
: Jl. Jakarta Blok BE No.24 RT.58 Loa Bakung Tlp : (0541) 270783
Samarinda Kalimantan Timur
BILKEV SERTIFIKASI INDONESIA
ISO 14001:2015 ISO 9001 :2015 ISO 45001:2018

DUTCH CONE PENETROMETER TEST

DCPT No. : S.04 (X:0529495; Y:9956267)
PROJECT : Uji Potensi Likuifaksi Daerah Samarinda
LOCATION : Jl. Hasanudin, Kel. Sungai Siring, Kota Samarinda
G. W. Level : -
Date Commenced : 20 September 2023
DCPT Type : Sondir Manual
Soil Test Technician : Supiansyah & Team
Soil Mec. Engineer : Isnawati Am.d

DEPTH (Meter)	Manometer Reading 1st M_1 (Kg/cm²)	Manometer Reading 2nd M_2 (Kg/cm²)	Compressive Strength Cone Resistance $M_1.C_2$ (Kg/cm²)	Compressive Strength Local Resistance $(M_2-M_1).C_1$ (Kg/cm²)	Total resistance $HL=(M_2-M_1).C_2.L/l$ (Kg/cm)	Accumulative JHL = ΣHL (Kg/cm)	Friction Ratio (%)
0,00	0,00	0,00	0,00	0,00000	0,00	0,00	0,00
20	20,00	25,00	19,78	0,43813	8,76	8,76	2,22
40	50,00	65,00	49,44	1,31440	26,29	35,05	2,66
60	85,00	105,00	84,05	1,75253	35,05	70,10	2,09
80	150,00	170,00	148,33	1,75253	35,05	105,15	1,18
1,00	256,00	281,00	253,15	2,19066	43,81	148,97	0,87
20							
40							
60							
80							
2,00							
20							
40							
60							
80							
3,00							
20							
40							
60							
80							
4,00							
20							
40							
60							
80							
5,00							
20							
40							
60							
80							
6,00							
20							
40							
60							
80							
7,00							
20							
40							
60							
80							
8,00							
20							
40							
60							
80							
9,00							
20							
40							
60							
80							
10,00							
20							
40							
60							
80							

Calculating the CSR (Cyclic Stress Ratio) Value

1) The first step is to compare the friction ratio and cone resistance values, as shown in **Figure 5**. The soil type value is obtained by looking at the soil type table in **Table 2**. After receiving the number of tanha type values, the soil type can be known through the soil type table in **Table 3** (Robertson, 2010).
2) Find the soil type by finding the value of soil specific gravity (γ), as seen in **Table 4**. Then, after obtaining the specific gravity of the soil, look at the saturated weight (γsat) and the pure weight of the soil (γdry).

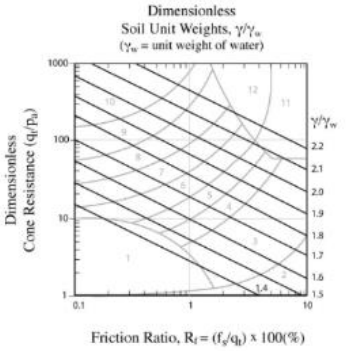

Figure 5. Comparison curve between cone resistance and friction ratio (Robertson, 2010).

Table 2. Table of soil types (Robertson, 2010)

Soil Behaviour Type (SBT)*	Approximate unit weight, γ (kN/m^3)
1	17.5
2	12.5
3	17.5
4	18.0
5	18.0
6	18.0
7	18.5
8	19.0
9	19.5
10	20.0
11	20.5
12	19.0

*SBT based on charts by Robertson et al., (1986)

Table 3. Parameter plot of the relationship between qc and soil type (Das, 2019)

Soil Type	Relative Density D_r, Percent	Standard Penetration Resistance N_{60} (Terzaghi and Peck 1967)	Cone Penetration Resistance q_c, ksf (Meyerhof 1974)	Friction Angle ϕ', deg		
				Meyerhof (1974)	Peck, Hanson and Thornburn (1974)	Meyerhof (1974)
Very Loose	< 20	< 4	----	< 30	< 29	< 30
Loose	20 - 40	4 - 10	0 - 100	30 - 35	29 - 30	30 - 35
Medium	40 - 60	10 - 30	100 - 300	35 - 38	30 - 36	35 - 40
Dense	60 - 80	30 - 50	300 - 500	38 - 41	36 - 41	40 - 45
Very Dense	> 80	> 50	500 - 800	41 - 44	> 41	> 45

Table 4. Plot of correction of density values with γ values (Terzaghi, 1948).

N SPT (blows/ft)	Konsistensi	q_u (Unconfined Compressive Strength) tons / ft^2	γ_{sat} kN/ m^3
< 2	Very soft	< 0,25	16 – 19
2 – 4	Soft	0,25 – 0,50	16 – 19
4 – 8	Medium	0,50 – 1,00	17 – 20
8 – 15	Stiff	1,00 – 2,00	19 – 22
15 – 30	Very stiff	2,00 – 4,00	19 – 22
> 30	Hard	> 4,00	19 – 22

3) Find the soil type by finding the value of soil specific gravity (γ), as seen in **Table 3**. Then, after obtaining the specific gravity of the soil, look at the saturated weight (γsat) and the pure weight of the soil (γdry).
4) Find the values of σv0 (total stress) and σv'0 (effective total stress)

$$\sigma v0 = (\sigma v0)n\text{-}1 + (\gamma dry\ .\ (h\text{-}hn\text{-}1)) \quad (1)$$

$$\sigma v'0 = (\sigma v0)n\text{-}1 + (\gamma dry\ \ (h\text{-}hn\text{-}1)) \quad (2)$$

5) Find the rd value or reduction stress coefficient

$$rd = \frac{(1000 - 0.4113z^{0.5} + 0.04052z + 0.001753z^{1.5}}{(1000 - 0.4177z^{0.5} + 0.05729z - 0.006205z^{1.5} + 0.00121z^{2}} \quad (3)$$

6) Calculating the CSR (Cyclic Stress Rasio)

$$CSR = 0.65\ (\frac{aMax}{g})\ (\frac{\sigma v0}{\sigma v'0}).\ Rd \quad (4)$$

7) Calculating the MSF

$$MSF = \frac{174}{M^{2.56}} \quad (5)$$

Calculating the CRR (Cyclic Resistance Ratio)

1) Convert qc and fs values into kpa from kg/cm²

$$qc = qc.\ 98.0665 \quad (6)$$

$$fs\ (Pa) = fs\ .\ 98.0665 \quad (7)$$

2) Calculating Cq

$$Cq = \left[\frac{Pa}{\sigma v'0}\right]^{n} \leq 1.7 \quad (8)$$

3) Calculating Q

$$Q = \left[\frac{qc - \sigma v0}{Pa}\right]\left[\frac{Pa}{\sigma v'0}\right]^{n} \quad (9)$$

4) Calculating F

$$F = \left[\frac{fs}{qc - \sigma v0}\right].\ 100\% \quad (10)$$

5) Calculating Ic

$$Ic = [(3.47 - logQ)^2 + (1.22 + logF)^2]^2 \quad (11)$$

6) Calculating Kc

$$Kc = -0.403Ic^4 + 5.581Ic^3 - 21.631Ic^2 + 33.75Ic - 17.88 \quad (12)$$

7) Calculating qc1N and qc1N(cs)

$$qc1N = Cq\left(\frac{qc}{Pa}\right) \quad (13)$$

$$(qc1N)cs = Kcqc1N \quad (14)$$

8) Calculating the CRR

$$CRR = 0.833.\left(\frac{qc1N}{1000}\right) + 0.05 \quad (15)$$

The safety factor value can be calculated by comparing the CRR value with CSR. The following is the formula for calculating FS.

Calculating safety factor (FS) and LPI values

$$FS = \frac{CRR}{CSR} \quad (16)$$

Table 5 LPI severity category

LPI	Iwasaki et al. (1982)
LPI = 0	Very low
0 < LPI < 5	Low
5 < LPI < 15	High
15 < LPI	Very high

After the calculation stage is carried out until the safety factor value is obtained, the LPI value can be determined and matched with the table, which can be seen in **Table 5**. The LPI value is calculated with the following equation:

$$\text{LPI} = \int_0^{20} f(z)w(z)dz \qquad (17)$$

2. Fuzzy-Gis Analysis

At this stage, the collected input data is processed. The data is processed through a computer or laptop. PGA (Peak Ground Acceleration), Vs30, groundwater table, lithology type, soil type, and slope are input data attributes processed with spatial data-based software such as ArcGIS. Furthermore, the weighting overlay and scoring methods are used to analyze each input data from the highest to the lowest. At this stage, the expected result is the type of liquefaction susceptibility modelling that can be applied to the study area. When all the spatial data has been analyzed, the Fuzzy-GIS method creates the modelling. Several input maps have been included to determine the liquefaction susceptibility zone. Some of these maps can be seen in **Figure 6**, and here are some of the input maps:

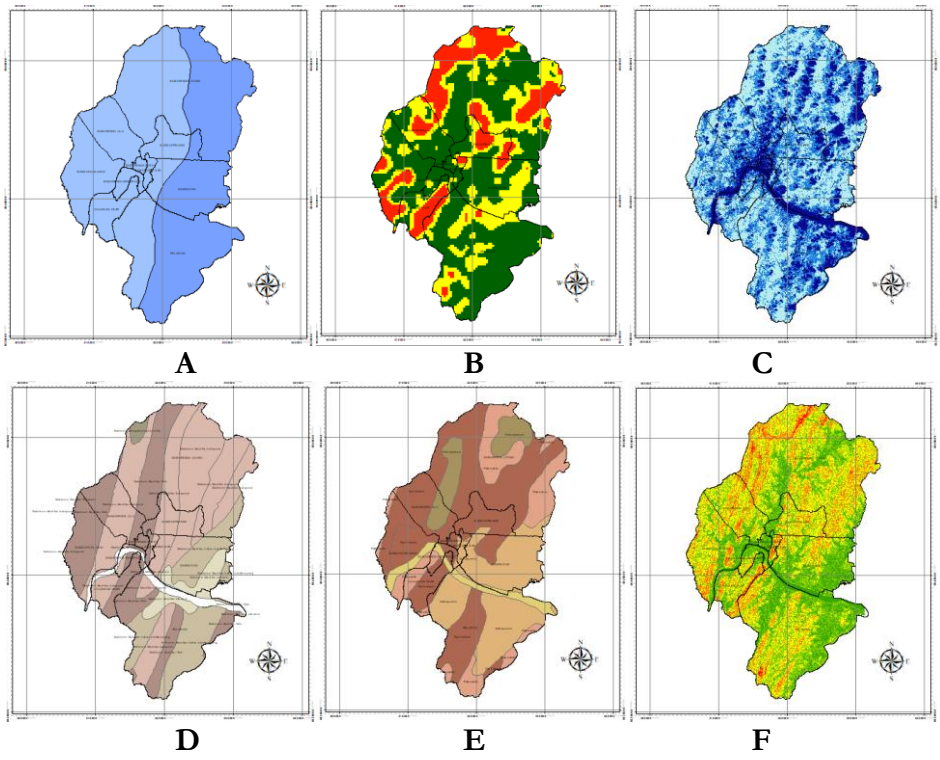

Figure 6. Map Input (A) PGA Map, (B) Vs30 Map, (C) Groundwater Potential Map. (D) LIthology Type Map, (E) Soil Type Map, (F) Slope Map

1. PGA Map

Pga maps are maps that depict the maximum ground acceleration during an earthquake. Pga is one of the critical parameters in determining seismic risk. The peak ground acceleration value is equivalent to the largest absolute acceleration amplitude recorded on the accelerogram at the earthquake site. In seismic engineering, peak ground velocity is an essential factor. Higher pga values indicate that more significant ground shaking occurs during an earthquake, meaning that buildings and structures in the area must be made more robust to survive. On the samarinda pga map, there are 2 pga values.

2. Groundwater Potential Map

Groundwater is water in the rock or subsoil below the surface from rainwater, snow, or other sources that enter the ground through gravity. Distinguish water-saturated and water-unsaturated aquifer zones. In simple terms, the water table is the depth at which the ground is saturated. Water-saturated zones are areas where soil pores and cracks are filled with water. Groundwater is also one of the factors that can influence liquefaction. Water in the soil cavities causes a high increase in hydrostatic pressure in the soil layers. Ground shaking and liquefaction can occur when the soil can no longer hold the groundwater together. The groundwater potential map of samarinda is divided into five zones, from very shallow to very deep.

3. Vs30 Map

A geophysical method that can detect shear wave propagation velocities up to 30 m depth (Vs30) is the Refraction Microtremor (ReMi) method, which records shear wave propagation occurring in the subsurface using sensor data from natural sources in the field. The Vs30 value is used to determine the classification of rocks based on the strength of earthquake vibrations due to local effects. With Vs30 input data that can be downloaded from PVMBG (Centre for Volcanology and Geological Hazard Mitigation), it can help determine liquefaction vulnerability zones more efficiently and accurately. Samarinda Vs30 map is divided into three classes, ranging from low to high.

4. Lithology Type Map

The type of rock lithology is one of the parameters that can affect the occurrence of liquefaction. Some rock types, such as sand and silt with loose grains, are prone to liquefaction. Areas composed of low-resistance rocks such as sandstones and siltstones are prone to landslides during ground movements because the existing constituent rocks are not strong enough to withstand cyclic loads, and existing ground movements make the constituent particles easily separated. At the same time, saturated water conditions can cause liquefaction in the area. Lithological types are divided into low, medium and high liquefaction potential—classes based on each region's nature and lithology types.

5. Soil Type Map

Soil types susceptible to liquefaction are loose sand to medium-saturated soils. Liquefaction only occurs in saturated soils, where pore water pressure is created by water between the soil pores. Soil type is an essential parameter in the liquefaction potential. Liquefaction usually occurs in sandy or loose-grained soils where the voids between the soil constituents are saturated with water. When high ground shaking occurs, certain types of soil saturated with groundwater will collapse and change phase from solid to liquid, which is then known as the phenomenon of liquefaction. Oil types are divided into three classes, namely low, medium and high liquefaction potential classes, based on each region's nature and characteristics of soil types.

6. Slope Map

Another factor that can cause liquefaction is slope. Areas with steep slopes are more susceptible to liquefaction, mainly if they are composed of low-resistance rocks and are dominated by granular soils such as silt or sand. When there are high-ground vibrations and the release of soil material due to the saturation of the water it contains, it can cause liquefaction. This result can be more severe in steep slopes, where liquefaction can spread widely and quickly to regions around the earthquake point. In the study area, there are five slope classes ranging from flat to very steep, as seen from the contour terrain of the region.

The next step in the Fuzzy-GIS analysis process is to input all the existing data and select the Fuzzy Product analysis type. The results of the Fuzzy Overlay Product analysis were then adjusted into four classes, namely very low, low, high, and very high liquefaction potential according to the LPI model created by (Iwasakil, 1982) and matched with the results of the CPT data calculation.

RESULT AND DISCUSSION

Result of Field Data Analysis

In the research area, there are 4 test location points spread across Samarinda City, which can be seen on the research location map. From the 4 test points, the CPT test data was obtained, which was then processed and analyzed using existing calculations to get the LPI value at each test point location. The following map of the research location is seen in **Figure 7**.

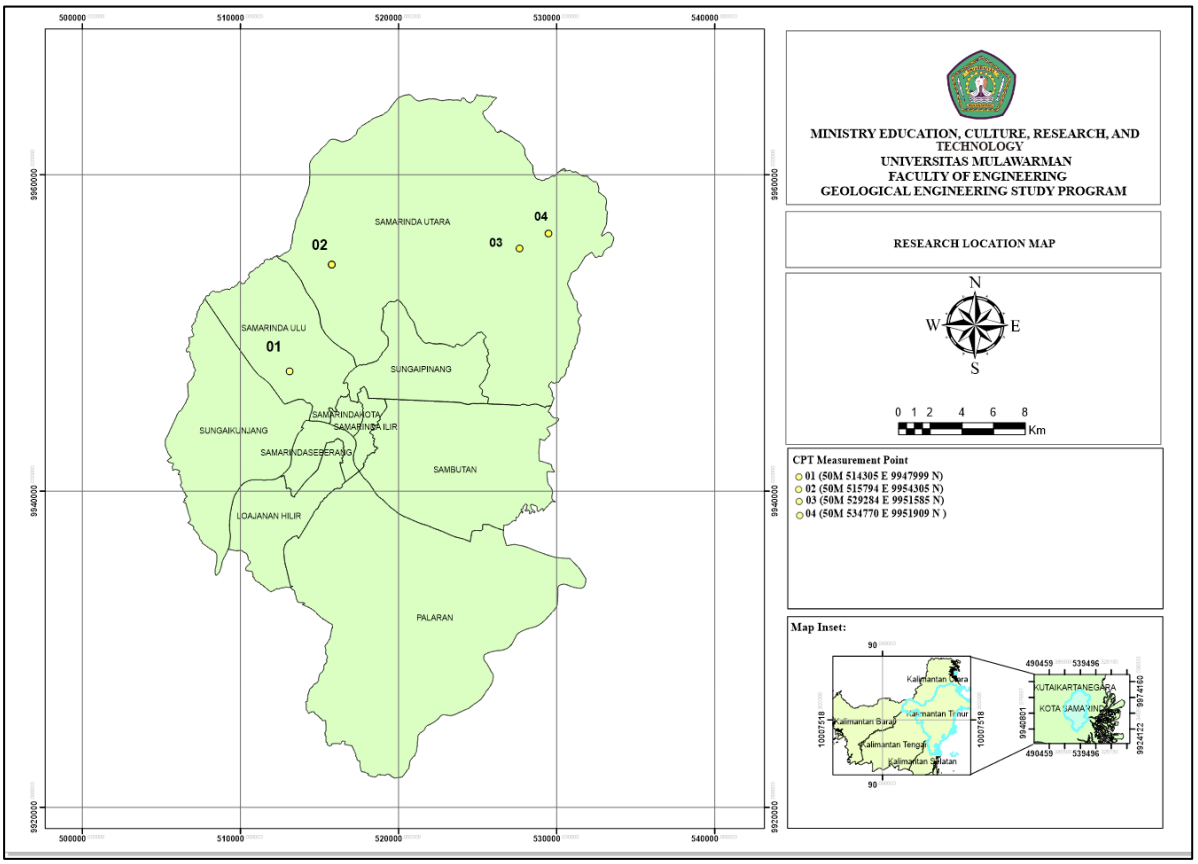

Figure 7. Cone penetration test (CPT) measurement location

1. At the first point, the CPT test location is at coordinates 513131°0'0 "E 9947546°0'0 "N in Air Putih Village, Samarinda Ulu Subdistrict, Samarinda City. At this point, the cones reach a depth of 7.4m. The following are the results of the LPI calculation at point 1 at a depth of 6m:

- **CSR**

  $\mathrm{CSR} = 0.65\ (\frac{aMax}{g})\ (\frac{\sigma v0}{\sigma v'0}).\mathrm{rd}$

  $\mathrm{CSR} = 0.65\ (\frac{59.5}{981})\ (\frac{84}{74.2}).0.96$

  $\mathrm{CSR} = 0.04$

- **CRR**

  $\mathrm{CRR} = 0.833.\left(\frac{qc1N}{1000}\right) + 0.05$

  $\mathrm{CRR} = 0.833.\left(\frac{65.18}{1000}\right) + 0.05$

  $\mathrm{CRR} = 0.1$

- **FS**

  $\mathrm{FS} = \frac{CRR}{CSR}$

  $\mathrm{FS} = \frac{0.04}{0.1}$

  $\mathrm{FS} = 2.43$

- **LPI**

  $\mathrm{LPI} = \int_0^{20} f(z)w(z)dz$

  $\mathrm{LPI} = \int_0^{20} 0\ .7$

  $\mathrm{LPI} = 0$

2. At the second point, the CPT test location is at coordinates 515794°0'0 "E 9954305°0'0 "N in North Sempaja Village, North Samarinda District, Samarinda City. At point 2, the cones reach a depth of 1.4m. The following are the results of the LPI calculation at point 2 at a depth of 1m:

- **CSR**

  $\mathrm{CSR} = 0.65\ (\frac{aMax}{g})\ (\frac{\sigma v0}{\sigma v'0}).\mathrm{rd}$

  $\mathrm{CSR} = 0.65\ (\frac{60.53}{981})\ (\frac{15.2}{15.2}).0.99$

  $\mathrm{CSR} = 0.04$

- **CRR**

  $\mathrm{CRR} = 0.833.\left(\frac{qc1N}{1000}\right) + 0.05$

  $\mathrm{CRR} = 0.833.\left(\frac{292.85}{1000}\right) + 0.05$

  $\mathrm{CRR} = 0.29$

- **FS**

  $\mathrm{FS} = \frac{CRR}{CSR}$

  $\mathrm{FS} = \frac{0.29}{0.4}$

$\mathrm{FS} = 7.40$

- **LPI**

  $\mathrm{LPI} = \int_0^{20} f(z)w(z)dz$

  $\mathrm{LPI} = \int_0^{20} 0\,.\,9.5$

  $\mathrm{LPI} = 0$

3. At the third point, the CPT test location is at coordinates 527674°0'0 "E 9955333°0'0 "N in Sungai Siring Village, North Samarinda Subdistrict, Samarinda City. At point 3, the cones reach a depth of 7m. The following are the results of the LPI calculation at point 3 at a depth of 4m:

- **CSR**

  $\mathrm{CSR} = 0.65\ (\frac{aMax}{g})\ (\frac{\sigma v0}{\sigma v'0}).\mathrm{rd}$

  $\mathrm{CSR} = 0.65\ (\frac{65.3}{981})\ (\frac{56}{56}).0.97$

  $\mathrm{CSR} = 0.04$

- **CRR**

  $\mathrm{CRR} = 0.833.\left(\frac{qc1N}{1000}\right) + 0.05$

  $\mathrm{CRR} = 0.833.\left(\frac{54.63}{1000}\right) + 0.05$

  $\mathrm{CRR} = 0.10$

- **FS**

  $\mathrm{FS} = \frac{CRR}{CSR}$

  $\mathrm{FS} = \frac{0.10}{0.04}$

  $\mathrm{FS} = 2.28$

- **LPI**

  $\mathrm{LPI} = \int_0^{20} f(z)w(z)dz$

  $\mathrm{LPI} = \int_0^{20} 0\,.\,8$

  $\mathrm{LPI} = 0$

4. At the fourth point, the CPT test location is at coordinates 529495°0'0 "E 9956267°0'0 "N in Sungai Siring Village, North Samarinda Subdistrict, Samarinda City. At point 4, the cones reach a depth of 1m. The following are the results of the LPI calculation at point 4 at a depth of 0.4m:

- **CSR**

  $\mathrm{CSR} = 0.65\ (\frac{aMax}{g})\ (\frac{\sigma v0}{\sigma v'0}).\mathrm{rd}$

  $\mathrm{CSR} = 0.65\ (\frac{65.92}{981})\ (\frac{6.2}{6.2}).1$

  $\mathrm{CSR} = 0.04$

- **CRR**

  $\mathrm{CRR} = 0.833.\left(\frac{qc1N}{1000}\right) + 0.05$

$$\text{CRR} = 0.833.\left(\frac{81.34}{1000}\right) + 0.05$$
$$\text{CRR} = 0.12$$

- **FS**

$$\text{FS} = \frac{CRR}{CSR}$$
$$\text{FS} = \frac{0.12}{0.04}$$
$$\text{FS} = 2.70$$

- **LPI**

$$\text{LPI} = \int_0^{20} f(z)w(z)dz$$
$$\text{LPI} = \int_0^{20} 0\,.9.8$$
$$\text{LPI} = 0$$

The calculation of the LPI value at each point of the existing CPT test location shows a value <1. From this existing value, if converted into a table of liquefaction severity (Iwasaki et al., 1982), it includes areas with very low liquefaction vulnerability.

Fuzzy Overlay Analysis Result

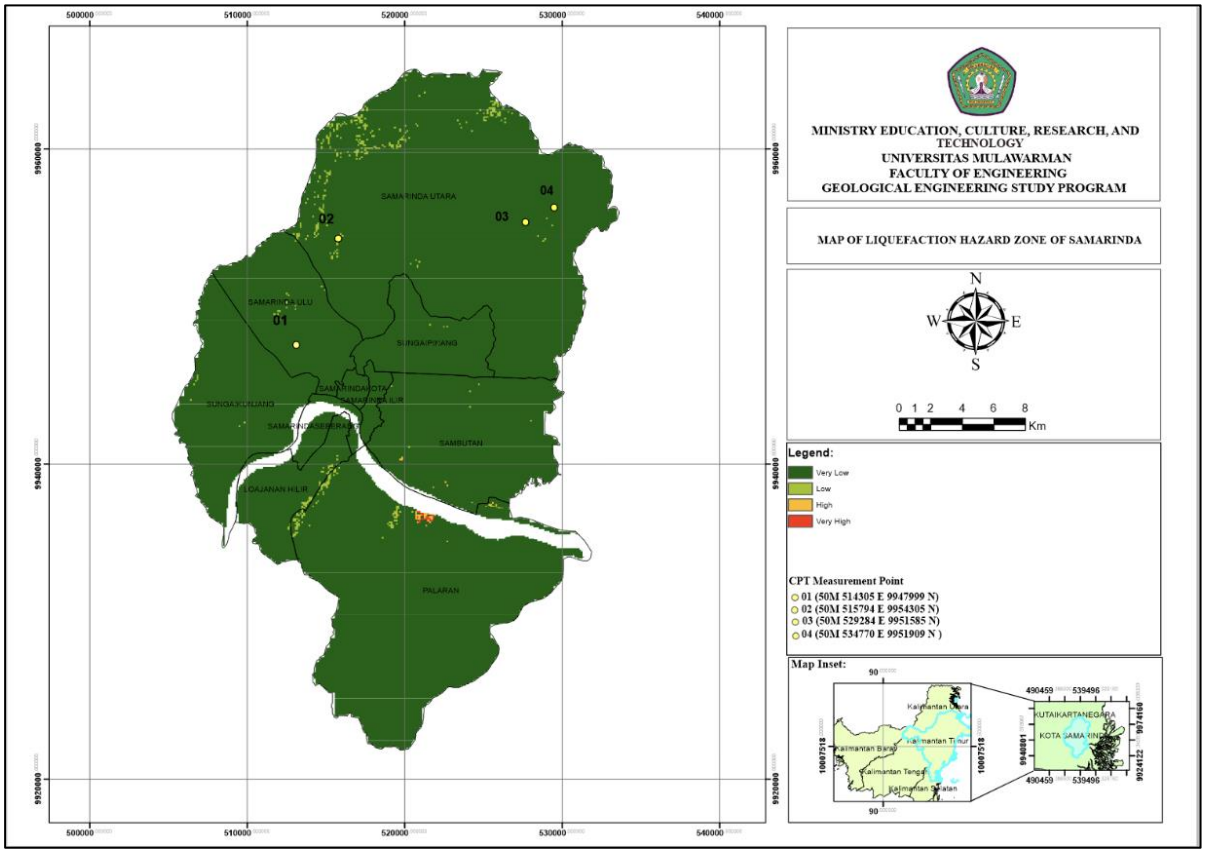

Figure 8. Map of the liquefaction hazard zone of Samarinda

In fuzzy overlay analysis, the operator chosen is a fuzzy overlay product. The fuzzy overlay product correctly analyzes the input data parameters to produce a liquefaction susceptibility zone, which can be proven by comparing the results of CPT calculations at four existing points, producing very low liquefaction potential results at these four points. Similarly, the fuzzy overlay product analysis showed shallow potential results at the four existing CPT test points. This condition proves that the liquefaction susceptibility zone map created is 100% accurate with the results of CPT field data. However, some areas have high liquefaction potential due to high input map values, such as PGA, vs30, groundwater potential, etc. The vulnerability zone model is divided into four zones, which can be seen in **Figure 8** as follows.

From the map of liquefaction vulnerability zones that has been made, it can be seen that several areas in Samarinda City have high liquefaction potential. This result is due to the type of Sulfaquents soil, which is coarse-grained, easily separated, and always in a water-saturated state. The next factor that causes high liquefaction potential is the type of alluvium lithology, which is sedimentary soil from the sedimentation process. Usually, this lithology has not been formed for a long time and has a low resistance level. The final factor that can cause high liquefaction potential is that the point has shallow groundwater potential, with steep slopes and high Vs30 acceleration values. Combining these factors can cause an area to have a high liquefaction potential.

The results of the fuzzy overlay analysis are 100% consistent and accurate with the results of the CPT data calculation in the field. This result can be seen from the 4 test points that both have shallow liquefaction potential values in fuzzy overlay analysis, and the results of CPT calculations in the field. The results of the distribution of liquefaction vulnerability zones in the research area are dominated by shallow liquefaction potential due to several factors, including the Palaran and Sambutan sub-districts of Samarinda City.

ACKNOWLEDGEMENTS

The authors thank the Geological Engineering Study Program Universitas Mulawarman for supporting this research. The Faculty of Engineering Universitas Mulawarman Research Grant funded this research with contract number 2673/UN17/HK.02.03/2023.

REFERENCES

Allen, G. P. & Chambers, J. L. (1998). Sedimentation in the Modern and Miocene Mahakam Delta. Jakarta, Indonesian Petroleum Association. (pp. 236).

Agung, P. A. M., Sultan, R., Idris, M., Sudjianto, A. T., Ahmad, M. A., & Hasan, M. F. R. (2023). Probabilistic of in Situ Seismic Soil Liquefaction Potential Based on CPT-Data in Central Jakarta, Indonesia. International Journal of Sustainable Construction Engineering and Technology, *14*(1), 241–248. https://doi.org/10.30880/ijscet.2023.14.01.021

Agustian, Y. (2021). Likuefaksi. In Yanyan Agustian Jurnal Ilmiah Teknologi Informasi Terapan (Vol. 8, Issue 1).

Arya Pranantya, P., Sukiyah, E., Prasetyo Utomo,) Edi, Hendarmawan,), Litbang, P., & Daya, S. (2018). Korelasi nilai sondir terhadap parameter geoteknik dan rembesan pada pondasi tanggul fase e, kalibaru, jakarta utara correlation of cone penetration test value to geotechnical parameters and seepage of e-phase ncicd seawall, kalibaru, north jakarta.

Boulanger, R. W., Idriss, I. M. (2014). Center for geotechnical modeling cpt and spt based liquefaction triggering procedures cpt and spt based liquefaction triggering procedures.

Darman, H. & Sidi, F. H. (2000). An outline of the geology of Indonesia. Jakarta, Ikatan Ahli Geologi Indonesia. (pp. 198).

Das, B. M. (2019). Advanced Soil Mechanics; Fifth Edition. CRC Press Taylor & Francis Group. New York.

Faizana, F., Laila Nugraha, A., & Darmo Yuwono, B. (2015). Pemetaan risiko bencana tanah longsor kota semarang. In Jurnal Geodesi Undip Januari (Vol. 4, Issue 1).

Fajarwati, Y., & Kusuma, R. I. (2021). Analisis Potensi Likuefaksi dan Perbaikan Tanah dengan Stone Column: Studi Kasus pada Coal Shelter PLTU Lontar, Banten. INERSIA: LNformasi Dan Ekspose Hasil Riset Teknik SIpil Dan Arsitektur, 17(1), 27–35. https://doi.org/10.21831/inersia.v17i1.40570.

Hakam, A. (2020). Analisis praktis potensi likuifaksi. ISBN: 978-623-7763-19-2. Andalas Press. Padang.

Hardianto, A., Winardi, D., Rusdiana, D. D., Putri, A. C. E., Ananda, F., Devitasari, Djarwoatmodjo, F. S., Yustika, F., & Gustav, F. (2020). Pemanfaatan Informasi Spasial Berbasis SIG untuk Pemetaan Tingkat Kerawanan Longsor di Kabupaten Bandung Barat, Jawa Barat. Jurnal Geosains Dan Remote Sensing, 1(1), 23–31. https://doi.org/10.23960/jgrs.2020.v1i1.16

Jalil, A., Fathani, T. F., Satyarno, I., & Wilopo, W. (2020). A study on the liquefaction potential in banda aceh city after the 2004 sumatera earthquake. International Journal of GEOMATE, *18*(65), 147–155. https://doi.org/10.21660/2020.65.94557

Indra, T., Sutjiningsih, D., Edhi Budhi Soesilo, T., & Kusratmoko, E. (2013). Gis Fuzzy Model For Assessing Vulnerability Of Water Resources In The Upper Citarum Watersheds (Issue 1). www.theinternationaljournal.org

Mase, Z., & Teoretis dan Terapan Bidang Rekayasa Sipil Jurnal Teoretis dan Terapan Bidang Rekayasa Sipil, J. (2017). Experimental Liquefaction Study of Southern Yogyakarta Using Shaking Table. 24(1). https://doi.org/10.5614/jts.2017.24.1.2.

Pusat Studi Gempa Nasional (2017). Peta Sumber dan Bahaya Gempa Indonesia Tahun 2017. Bandung, Kementerian Pekerjaan Umum dan Perumahan Rakyat. (pp. 376).

Robertson, P. k. (2010). Estimating soil unit weight from CPT. 2nd Internasional Symposium on Cone Penetration testing, Huntington Beach, CA, US. California. USA.

Santoso, H., Ssop Bantal, A. ", Das, B., Banjir, P., Longsor, T., & Penanggulangan Bencana, J. (2012). Aplikasi "ssop bantal" berbasis das untuk penanggulangan banjir dan tanah longsor (Vol. 3, Issue 1).

Terzaghi, K. and Peck, R.B., 1948, Soil Mechanics in Engineering Practice, Wiley, New York.

Wijayanto, A. G. (2020). Pemodelan Rekomendasi Tempat Pembungan Sampah Sementara Menggunakan FUZZY OVERLAY Di Kabupaten Semarang.Jurnal Sistem Informasi, Vol.9: 27-35. 571-1916-4-PB. Universitas Kriten Satya Wacana. Salatiga.

Yassar, M. F., Nurul, M., Nadhifah, N., Sekarsari, N. F., Dewi, R., Buana, R., Fernandez, S. N., & Rahmadhita, K. A. (2020). Penerapan Weighted Overlay Pada Pemetaan Tingkat Probabilitas Zona Rawan Longsor di Kabupaten Sumedang, Jawa Barat. Jurnal Geosains Dan Remote Sensing, 1(1), 1–10. https://doi.org/10.23960/jgrs.2020.v1i1.13

Zeffitni, Basir-Cyio, M., Napitupulu, M., & Worosuprojo, S. (2020). Spatial analysis of the liquefaction vulnerability zone based on the phreatic level at the Palu groundwater basin, Central Sulawesi Province. Journal of Physics: Conference Series, 1434(1). https://doi.org/10.1088/1742-6596/1434/1/012019